NASA TECHNICAL MEMORANDUM

NASA TM X-71449

NASA TM X-71449

FLAP NOISE PREDICTION METHOD FOR A POWERED LIFT SYSTEM

by B. Clark, R. Dorsch, and M. Reshotko
Lewis Research Center
Cleveland, Ohio 44135

TECHNICAL PAPER proposed for presentation at
Aero-Acoustic Specialists Conference sponsored by
the American Institute of Aeronautics and Astronautics
Seattle, Washington, October 15-17, 1973

FLAP NOISE PREDICTION METHOD FOR A POWERED LIFT SYSTEM

by B. Clark,[1] R. Dorsch,[2] and M. Reshotko[3]
V/STOL and Noise Division
Lewis Research Center
National Aeronautics and Space Administration
Cleveland, Ohio

E-7717

Abstract

A method is presented for estimating the noise generated by deflection of the engine exhaust for under-the-wing and over-the-wing versions of an externally blown flap configuration for powered lift. Correlation equations and curves are given for the OASPL and directivity and for spectra scaled to a high bypass 25 000-pound thrust size engine. Data are taken from TF34 engine tests and from large cold flow model tests. The correlations are empirical, and thus application of this prediction procedure is limited to geometrically similar configurations. Application of the method is illustrated by calculated sample footprints.

Introduction

Current interest in aircraft for short-haul applications includes those utilizing externally blown flaps for powered lift. The nature of the operation of such aircraft, as well as the possibility of more restrictive noise goals, require that they be considerably quieter than conventional (CTOL) aircraft. The noise resulting from the powered lift can be the dominant noise source. For the externally blown flap (EBF) configurations, noise is produced as the engine exhaust flows over either the upper or lower surfaces of the wing-flap system. This noise is referred to herein as "flap" noise; it includes leading and trailing edge noise, scrubbing noise, and redirected jet noise.

Extensive data for flap noise have been obtained recently in both cold flow model tests and tests with an actual engine. Results of these tests are being reported separately.[1-8] Noise considerations in aircraft design require correlation of these fragmentary data and a method of making consistent noise predictions.

The method of flap noise prediction of this paper consists of equations and curves for overall sound pressure level and directivity and spectrum shape. By means of these, the spectrum of flap noise, or the perceived noise level, can be predicted for any distance and for a range

---

[1] Aerospace Engineer, Applications Analysis Office.

[2] Head, Section B, Jet Acoustics Branch.

[3] Aerospace Engineer, Jet Acoustics Branch.

of direction angles from the source. Sample footprints for under-the-wing and over-the-wing configurations are presented to illustrate the results of this prediction method.

Data Sources

The curves and equations for predicting the flap noise are based primarily on data from two sources: TF34 engine tests[1-3] at the NASA Flight Research Center; and large cold flow model tests at the Lewis Research Center.[4-6] Both tests were conducted using under-the-wing (UTW) and over-the-wing (OTW) configurations. Small-scale (2-in. nozzle diam.) cold flow test data reported in references 5 and 7 are used for comparison to help in interpreting the large model and engine test results.

Geometrical relations of the engine, wing, and flaps used in the TF34 engine tests are shown in figures 1 and 2 for UTW and OTW configurations. Fan and internal core noise were highly suppressed,[1] leaving the flap noise as the dominant noise source. In the UTW configurations, data were taken with a separate-flow (coannular) nozzle at flap angles, ψ, of 0°, 40°, and 55°, where the flap angle refers to the trailing flap. In the OTW configuration, noise data were taken with an internal mixer nozzle on the engine exhaust, and with a simulated flap angle of 40°. A deflector was used on the engine exhaust for the OTW case to obtain good flow attachment to the flap upper surface. The aspect ratio of the wing section tested was about one.

Large model data were obtained in tests with a conical or a coannular nozzle fed from a muffled cold air supply. Both UTW and OTW configurations, shown in figures 3 and 4, were tested. Flap angles were 0°, 20°, and 60°. The coannular nozzle (fig. 3(a)) was roughly a one-half scale model of the TF34 separate flow nozzle of figure 1. The wing section aspect ratio was 1.3.

The test configurations for which data were used for this paper are summarized in Table I. The range of effective exhaust velocities used in the correlations is listed for each test configuration ("effective" velocity will be defined later). Data were not available for all test variables.

Approach

It is desired to predict the perceived noise level in PNdB due to flap noise at some point in the noise field, or at a series of points for a noise footprint. These calculations require a knowledge of the one-third octave band sound pressure level (SPL) spectra for the configuration of interest. The prediction method for these spectra as developed herein contains a number of steps.

The procedure chosen starts with the prediction of the flap noise OASPL in one direction (the reference direction) by equations involving

TABLE I. - RANGE OF TEST VELOCITY (fps)

Configuration		TF34 engine tests				Large model cold flow tests			
		Nozzle	Flap angle			Nozzle	Flap angle		
			0°	40°	55°		0°	20°	60°
Under-the-wing	Flyover plane	Separate flow	540-820	540-830	540-820	Coannular	415-810	470-870	465-870
	Sideline*		545-760	540-830	540-820		-	-	465-810
	Flyover plane					Convergent	-	570-830	570-830
	Sideline*						-	-	-
Over-	Flyover plane	Converg. mixed flow; deflector	-	510-780	-	Convergent with deflector	-	620-830	630-830
							-	620-830	-
	Sideline*		-	510-780	-				

*In the plane perpendicular to the engine axis (within 10 degrees).

the distance from the flap, the flap angle, the nozzle area, and the effective exhaust velocity. Curves of OASPL directionality are then presented so that adjustment to the reference OASPL can be made for levels in other directions.

In the final step of the development, curves are presented for normalized one-third octave SPL spectra. The normalized spectra relate the OASPL and the spectrum band levels frequency-scaled to a reference EBF configuration.

Correlations

Directly beneath the aircraft is chosen as the reference direction (fig. 5) for the determination of the reference OASPL. Overall sound pressure levels in this direction ($OASPL_{REF}$) show a sixth-power dependence on nozzle exhaust velocity and a first power dependence on nozzle area, as in reference 8. Directionality of the noise in OASPL is given in terms of the projected angles θ in the flyover plane and ϕ in the plane perpendicular to the engine axis, as defined in figure 5. Values of OASPL presented have all atmospheric attenuation removed (i.e., lossless).

Test results at a point at distance R from the flap system are correlated by the equation

$$OASPL_{REF} = K + 10 \log \left(\frac{A}{A_o}\right)\left(\frac{R_o}{R}\right)^2 + 60 \log \left(\frac{V_{EFF}}{V_o}\right) \qquad (1)$$

where $OASPL_{REF}$ is the overall sound pressure level in the geometric reference direction ($\theta = 90^o$, $\phi = 0^o$) at the same distance. The nozzle has a total exhaust area A and effective exhaust velocity V_{EFF}. The parameter K depends on the configuration, as will be discussed later. The OASPL are referenced to 0.2 nanobar. Constants chosen for the equation are

$$A_o = 1.0 \text{ sq ft}$$

$$R_o = 100 \text{ ft}$$

$$V_o = 500 \text{ ft/sec}$$

A noise weighted average of the exhaust velocities impinging on the flap surface would be the best effective velocity for correlation purposes. These impingement velocities are generally unavailable and difficult to calculate. Therefore, for nozzles with a low velocity decay rate, a weighted average velocity at the nozzle exit is used as the effective velocity for the correlation. This weighted average varies according to the type of nozzle used.

For the separate flow nozzle used on the TF 34 and the large model coannular nozzle, which have essentially unmixed flows at the exit, the noise weighted average for the effective velocity is expressed by

$$V_{EFF} = \left(\frac{A_C V_C^6 + A_F V_F^6}{A_C + A_F}\right)^{1/6} \qquad (2)$$

where the subscripts F and C refer to the fan and core flows, respectively, and the component velocities are the ideal fully expanded velocities at each nozzle exit. In the TF34 tests the velocity ratio V_C/V_F varied from 1.29 at 100 percent speed to 0.98 at low speed. Typical velocity ratios in the large model tests with the coannular nozzle were from 1.22 at higher velocities to 1.48 at low velocities. However, OASPL from both sets of UTW tests were well correlated by the effective velocity of equation (2). They also correlated well with the OASPL from UTW tests with a convergent nozzle, where the effective velocity was taken as the ideal expanded velocity at the nozzle exit.

In the case of an internal mixer-type nozzle, such as was used in the OTW TF34 tests, a mass-average velocity was used, defined by

$$V_{EFF} = \frac{BPR\ V_F + V_C}{BPR + 1} \tag{3}$$

where BPR is the mass-flow bypass ratio. Based on this definition of effective velocity, the OASPL from the OTW TF34 tests correlate well with the OASPL from the large model OTW tests with a simple convergent nozzle.

In the case of the flap setting of 0^o with the separate flow and coannular nozzles, the effective velocity was taken equal to the fan exhaust velocity, under the assumption that the core flow did not strike the wing or retracted flaps.

For the correlations in this paper, the range of effective exhaust velocities was between 415 and 870 feet per second, as indicated in Table I.

Under-the-wing configurations

Although the parameter K (eq. (1)) varies with flap angle, nozzle position, and relative size with respect to the wing and flaps, for the specific geometries of figures 1 and 3 only the flap angle dependence will be considered. Values of K for use in the UTW configurations are shown in figure 6 to be approximated to within ±1.5 dB by

$$K = 86.5 + 0.14\ \psi \tag{4}$$

where ψ is the angle in degrees between the trailing flap and the mean chord line of the wing (fig. 5). The TF34 data are slightly higher than this prediction, while the large model data are about one decibel lower than the line. Figure 6 illustrates also the excellent correlation of the OASPL data obtained with the sixth power of the effective velocities, and by the type of weighted average used for the effective velocities for coannular and convergent nozzles.

Directivity. Directivity curves for the UTW flap noise are shown in figure 7. From these curves OASPL can be predicted for directions other than the reference direction by the equation

$$OASPL_{\theta,\phi} = OASPL_{REF} + \Delta_\theta + \Delta_\phi \tag{5}$$

Flaps at the high angle (ψ) settings show the most directivity effect in both θ and ϕ directions. Jet noise at the higher velocities apparently begins to contribute to the θ directivity causing the noise to shift somewhat from the forward to rear quadrants in θ. This effect appears as scatter in the Δ_θ data and is neglected in the recommended curves.

Comparison of the Δ_ϕ values based on TF34, large model, and small

model tests shows considerable scatter at $\phi = 90^{\circ}$. For flap angles of 55° and 60°, $\Delta_{\phi=90}$ scatters ±3.5 dB for the three sets of tests. The scatter in Δ_{ϕ} is greater than in Δ_{θ}.

The Δ_{θ} and Δ_{ϕ} curves as drawn are composites of the data and represent, in the opinion of the authors, the best averages of the data available at this stage with flap noise experiments.

Normalized spectra. One-third octave SPL spectra from TF34 engine and large model tests were frequency scaled to a 74-inch equivalent diameter nozzle (30 sq ft total exhaust area) chosen as typical for a 25 000-pound thrust engine for short-haul aircraft. Effects of atmospheric attenuation were removed from all of the spectra to make them lossless. In addition, the spectra were smoothed to remove cancellations and reinforcements due to ground reflections.

The recommended spectrum shapes for use for the UTW configuration in the flyover plane ($\phi = 0^{\circ}$) and in the wingtip sideline direction ($\phi = 90^{\circ}$) are shown in normalized form in figure 8. A linear interpolation may be used for spectrum shapes at intermediate ϕ angles. The spectrum shape for the flyover plane correlates the available data within ±3 dB for all flap angles and for θ between 40° and 120°, where the flap noise tends to be dominant. The recommended spectrum shape in the wingtip sideline direction is somewhat flatter than that in the flyover plane. At high frequencies the flyover spectrum falls off at 4.2 dB per octave, and the wingtip sideline spectrum falls off at 3.4 dB per octave.

For applications at other thrust size or nozzle size, the spectra of figure 8 must be frequency scaled inversely with diameter to the desired nozzle size. Although flap noise spectra shift with velocity, as was shown in reference 4, this shift was ignored because, for the range of exhaust velocities covered (415 to 870 fps), it was within the scatter band in the data due to other effects.

Nozzle position and diameter. If the nozzle relative position and diameter are significantly different from those shown in figures 1 and 3, the K values should be modified. An indication of the sensitivity of K to these differences can be drawn from the TF34 tests and small model tests.[7,8] Generally, noise levels (and K) decrease slowly for nozzle relative displacement in the forward direction $\theta = 0^{\circ}$, and rapidly for displacement in the downward direction $\theta = 90^{\circ}$. For example, advancing the TF34 engine in the direction $\theta = 0^{\circ}$ by a distance 2/3 of an equivalent diameter resulted in 0.9 dB decrease in K. Lowering the engine in the direction $\theta = 90^{\circ}$ by 0.24 diameters decreased K by 2.1 dB.

The parameter K is not very sensitive to changes in the relative nozzle size. The data of reference 7 indicate a 1.4 dB increase in K for a diameter increase of 50 percent. Reference 8 indicates that for constant wing and flap size, OASPL (and K) are approximately proportional to 10 log D. However, the trends with nozzle position and diam-

eter discussed in this section are based on meager data, and no specific correction factors are proposed.

Over-the-wing configurations

The values of K obtained from the data for the OTW configurations of the TF34 and large model tests (figs. 2 and 4, respectively) are shown in figure 9. The average line through the experimental values is

$$K = 87 + 0.01\,\psi \tag{6}$$

within ±1 dB. Data from TF34 tests were available only at a flap angle of 40°. Large model data were for 20° and 60° flap angles. No data were available for flaps at $\psi = 0^\circ$, so the prediction is only reliable from $\psi = 20^\circ$ to 60°. The small spread in the values of K indicates that the data are well correlated by the recommended effective velocities and by a sixth power velocity dependence, as the UTW data were (fig. 6).

Directivity. OTW directivity factors for equation (5) for OASPL in the θ and ϕ planes are given in figure 10. A minimum occurs in the ϕ plane between low ϕ angles where low frequency trailing edge noise predominates, and $\phi = 90^\circ$ where the high frequencies above the wing are only partly shielded. In the ϕ plane the only data available were at a 20° flap angle for the large model tests and 40° flap angle for the TF34 tests. As in the UTW case, the θ directivity in the flyover plane shifts more toward the rear quadrant with increasing velocity, but this effect is neglected in the recommended curves.

Normalized spectra. Normalized one-third octave spectrum shapes for OTW configurations are given in figure 11. It is recommended that the flyover spectrum shapes be used for ϕ angles out to 65°. Interpolated shapes should be used from $\phi = 65^\circ$ to 90°. In the θ plane, the flyover spectrum shape is valid for θ from 50° to 120°.

Applications

Calculation procedure

The relations for $OASPL_{REF}$, directivity curves, and recommended normalized spectrum shapes can be used to construct 1/3-octave SPL spectra of flap noise at an observer point at distance R in a direction defined by θ and ϕ for a given EBF system.

The geometrical relationships between an observer position and the aircraft position and attitude at some instant in time must first be solved to define the observer position in R, θ, and ϕ with respect to the aircraft as defined in figure 5 (values of θ must be within the prescribed range for a valid prediction). From the engine size and type, the proper values of areas and velocities must be chosen to calculate an effective velocity. For an UTW or OTW configuration, K is then calcu-

lated for the correct flap angle from equation (4) to (6), and $OASPL_{REF}$ is calculated by equation (1) for the distance R. The appropriate directivity factors in Δ_θ and Δ_ϕ are applied as in equation (5) to find the OASPL at the observer location (R, θ, ϕ). The selection of the appropriate spectrum shape, with interpolation as directed and frequency-scaling if required, allows the calculation of the 1/3-octave SPL spectrum at the observer location when the aircraft is at the specified location.

Various corrections must be made to this spectrum. These include the effects of multiple engines, atmospheric attenuation for the distance R, ground reflections, fuselage or engine shielding, and extra ground attenuation. Corrections for small variations from the reference nozzle-wing-flap geometry may also be made, if data are available.

For total system noise, the corrected flap noise spectrum is combined with corrected spectra from other sources, e.g., engine noise. The perceived noise level (PNdB) is calculated from the combined spectrum. For calculating aircraft PNL footprints, the above calculations are repeated for a range of aircraft positions along its flight path with respect to each of a matrix of observer positions.

Sample calculations.

As a simple example, PNL footprints of flap noise only are shown in figure 12. The footprints are for a single engine with 30° flap angle in both UTW and OTW configurations. The aircraft path is a simulated take-off with a 10° climb angle and a 10° angle of attack. Assumed velocities and areas for the UTW configuration are 750 fps and 5 sq ft for the core, and 650 fps and 25 sq ft for the fan exhaust. For the OTW case, a mixed velocity of 673 fps and nozzle area of 30 sq ft were assumed.

For these calculations correction was made only for atmospheric attenuation. No allowances were made for extra ground attenuation, fuselage shielding, or forward velocity effects. The initial wide portion of the OTW footprint occurs at very low aircraft altitude and would largely disappear if extra ground attenuation were included.

Concluding Remarks

A method of predicting flap noise has been developed, based on acoustic tests with specific jet exhaust, wing, and flap geometries. The method is relatively simple and capable of producing acceptable preliminary results for configurations similar to those contained in the analysis.

Further testing is needed to predict the effects of any major configurational changes. In the configurations already tested, there is need for more acoustic data, especially in the OTW case and for the sideline noise levels in both UTW and OTW cases. The effects of wing aspect ratio on sideline directivity also need to be explored. In addition, other ef-

fects, which were not included in this method, such as spectrum shape changes with velocity, can perhaps be included in the prediction. As more data becomes available, the user should update the relations used in this paper.

References

1. Jones, W. L., Heidelberg, L. J., and Goldman, R. G., "Highly Noise Suppressed Bypass 6 Engine for STOL Applications," Paper 73-1031, Oct. 1973, AIAA, New York, N.Y.

2. Samanich, N. E., Heidelberg, L. J., and Jones, W. L., "Effect of Exhaust Nozzle Configuration on Aerodynamic and Acoustic Performance of an Externally Blown Flap System with a Quiet 6:1 Bypass Ratio Engine," Paper 73-1217, Nov. 1973, AIAA, New York, N.Y.

3. Dorsch, R. G., and Reshotko, M., "EBF Noise Tests with Engine Under and Over the Wing Configurations," STOL Technology, SP-320, 1973, NASA, Washington, D.C.

4. Dorsch, R. G., Kreim, W. J., and Olsen, W. A., "Externally-Blown-Flap Noise," Paper 72-129, Jan. 1972, AIAA, New York, N.Y.

5. Dorsch, R. G., Reshotko, M., and Olsen, W. A., "Flap Noise Measurements for STOL Configurations Using External Upper Surface Blowing," Paper 72-1203, Nov. 1972, AIAA, New York, N.Y.

6. Reshotko, M., Goodykoontz, J. H., and Dorsch, R. G., "Engine Over-the-Wing Noise Research," Paper 73-631, July 1973, AIAA, New York, N.Y.

7. Olsen, W. A., Dorsch, R. G., and Miles, J. H., "Noise Produced by a Small-Scale Externally Blown Flap," TN D-6636, 1972, NASA, Cleveland, Ohio.

8. Dorsch, R. G., Lasagna, P. L., Maglieri, D. J., and Olsen, W. A., "Flap Noise," Aircraft Engine Noise Reduction, SP-311, 1972, NASA, Washington, D.C., pp. 259-290.

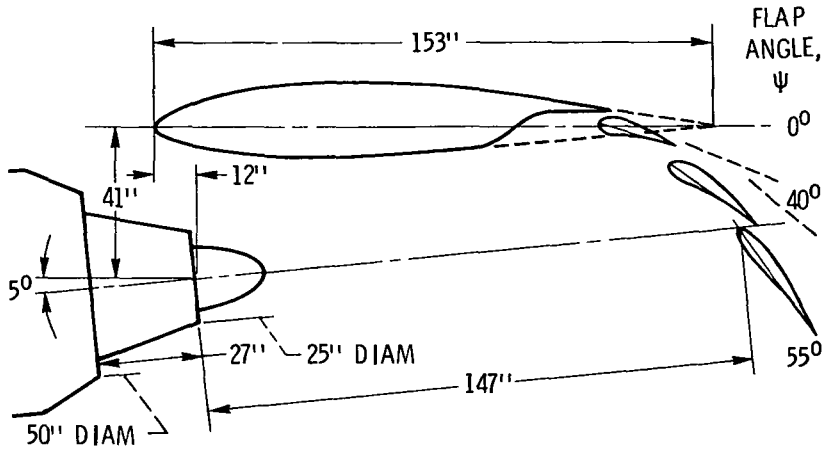

Figure 1. - Sketch of TF 34 engine under-the-wing test configuration. Core exhaust area is 280 sq in., fan exhaust area is 790 sq in.

E-7717

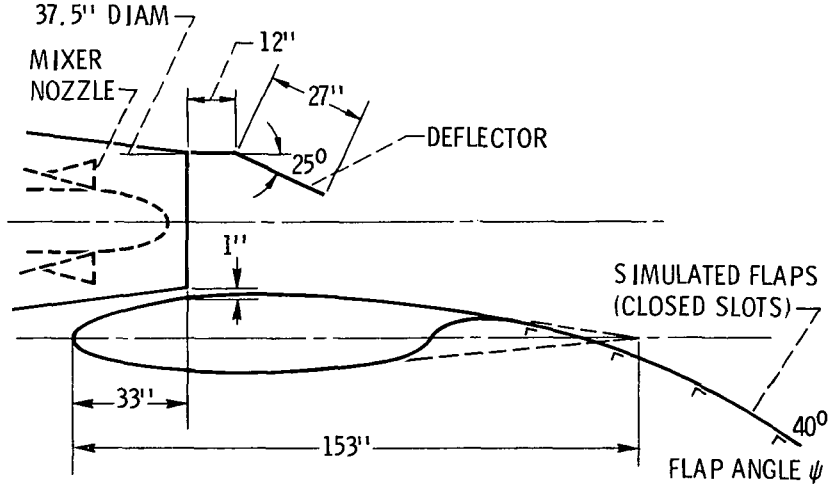

Figure 2. - Sketch of TF 34 engine over-the-wing test configuration, including the internal mixer and external flow deflector. Exhaust nozzle area is 1104 sq in.

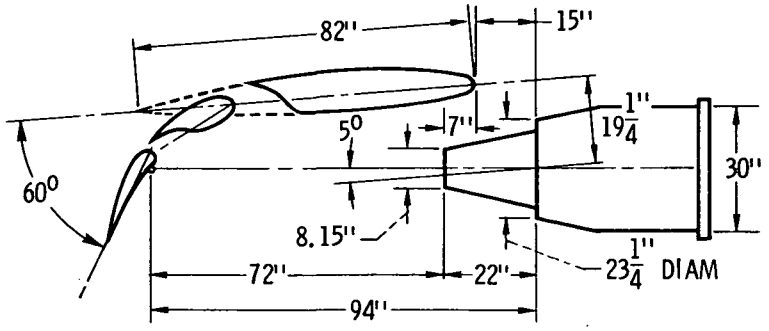

(A) WITH CO-ANNULAR NOZZLE; CORE EXHAUST AREA IS 51.8 SQ IN. ANNULAR EXHAUST AREA IS 169.9 SQ IN.

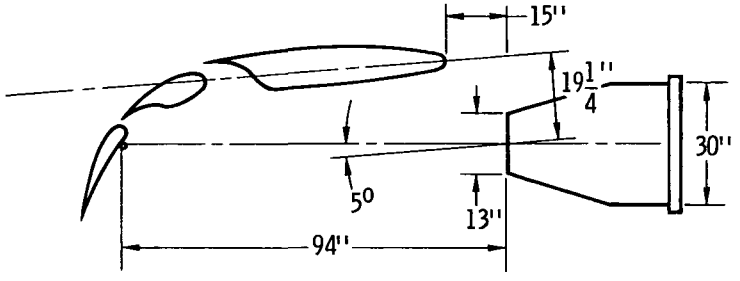

(B) WITH 13-INCH-DIAMETER CONVERGENT NOZZLE; EXHAUST AREA IS 132.7 SQ IN.

Figure 3. - Under-the-wing configurations for cold flow tests with large externally blown flap model; 60° flap angle shown.

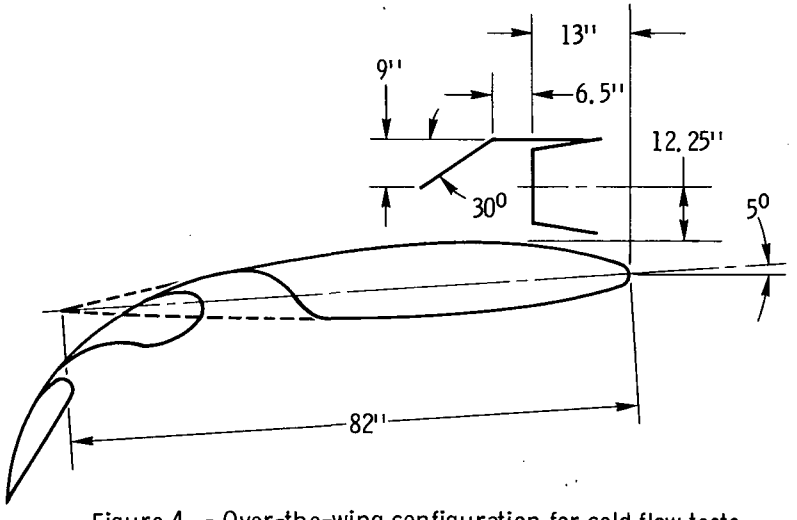

Figure 4. - Over-the-wing configuration for cold flow tests with large flap model, 13-inch diameter convergent nozzle and deflector. Flap slots are covered, 60° flap angle shown.

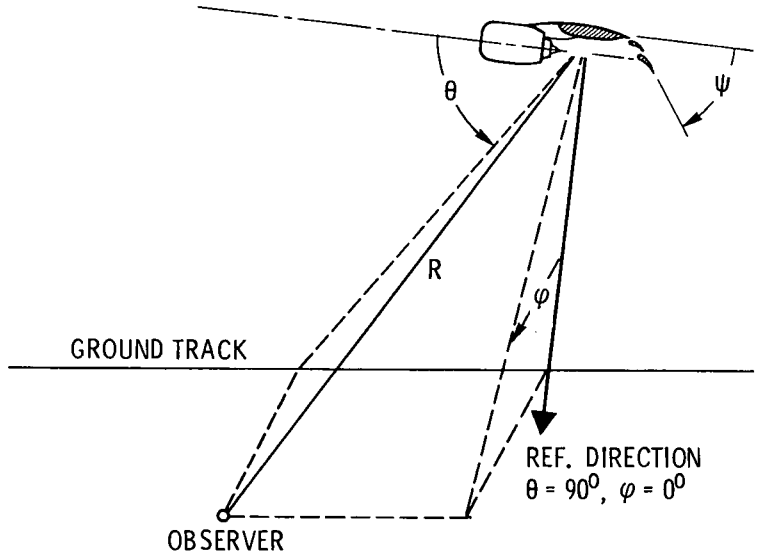

Figure 5. - Angle geometry for flap noise directivity.

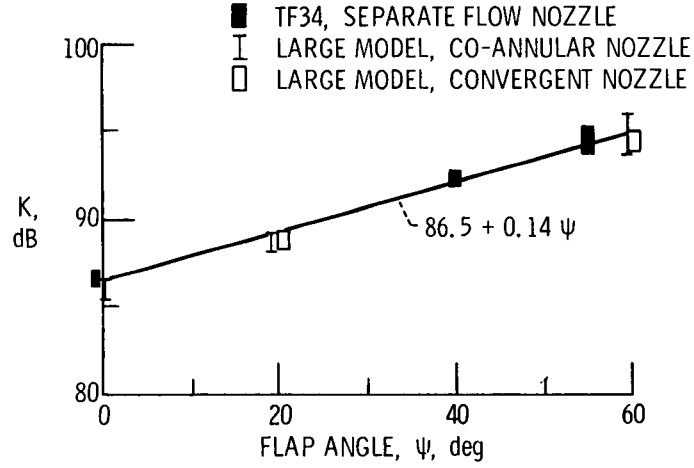

Figure 6. - Variation of K (eq. (4)) with flap angle for under-the-wing TF34 and large model tests. Scatter in K over the velocity range is indicated.

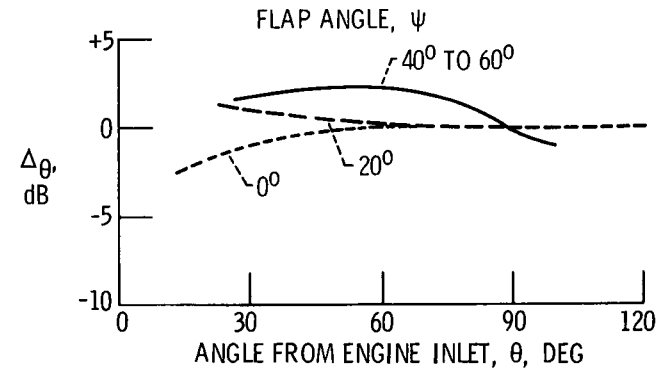

(a) FLYOVER PLANE, $\varphi = 0^{\circ}$. $\Delta_{\theta} = OASPL_{\theta} - OASPL_{REF}$

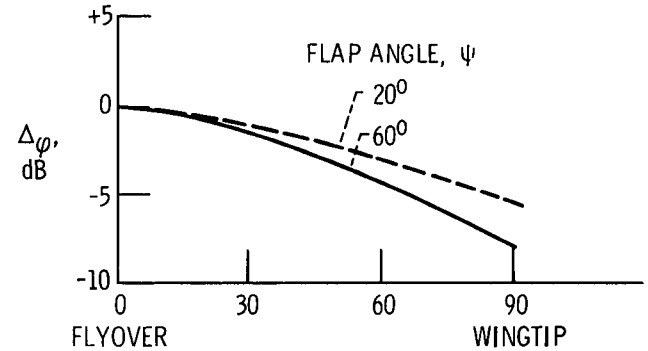

(b) PLANE PERPENDICULAR TO ENGINE AXIS, $\theta = 90^{\circ}$. $\Delta_{\varphi} = OASPL_{\varphi} - OASPL_{REF}$

Figure 7. - Under-the-wing flap noise directivity at a constant radius.

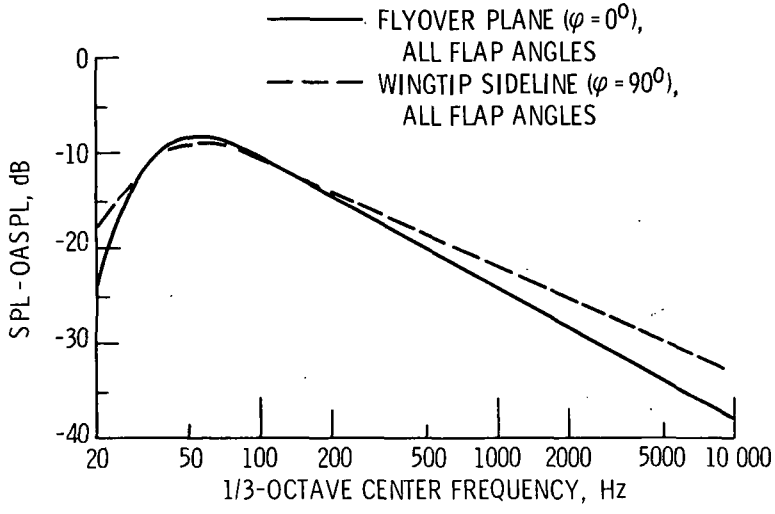

Figure 8. - Under-the-wing normalized flap noise spectra, scaled to nominal 25 000-pound thrust size (74-in. equivalent nozzle diameter), for θ from 40° to 120°.

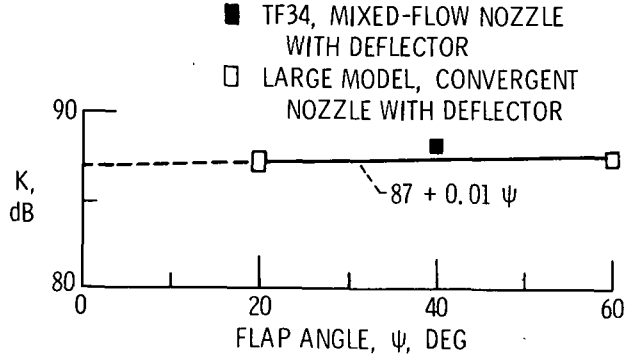

Figure 9. - Variation of K (eq. (6)) with flap angle for over-the-wing TF34 and large model tests. Scatter in K over the velocity range is indicated.

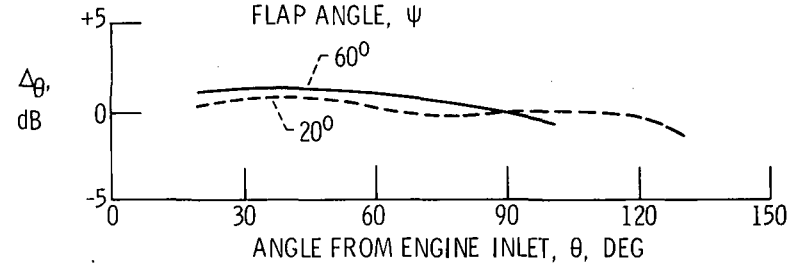

(a) FLYOVER PLANE, $\varphi = 0^{\circ}$. $\Delta_{\theta} = OASPL_{\theta} - OASPL_{REF}$

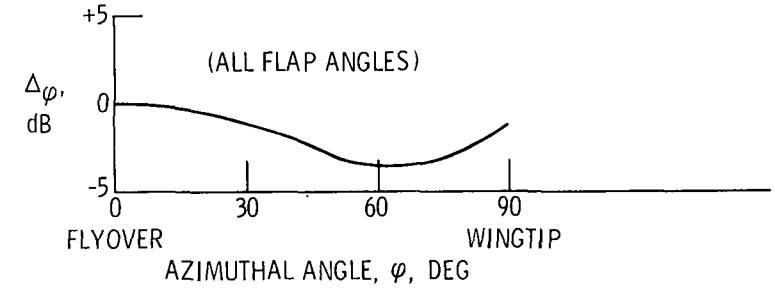

(b) PLANE PERPENDICULAR TO ENGINE AXIS, $\theta = 90^{\circ}$. $\Delta_{\varphi} = OASPL_{\varphi} - OASPL_{REF}$

Figure 10. - Over-the-wing flap noise directivity at a constant radius.

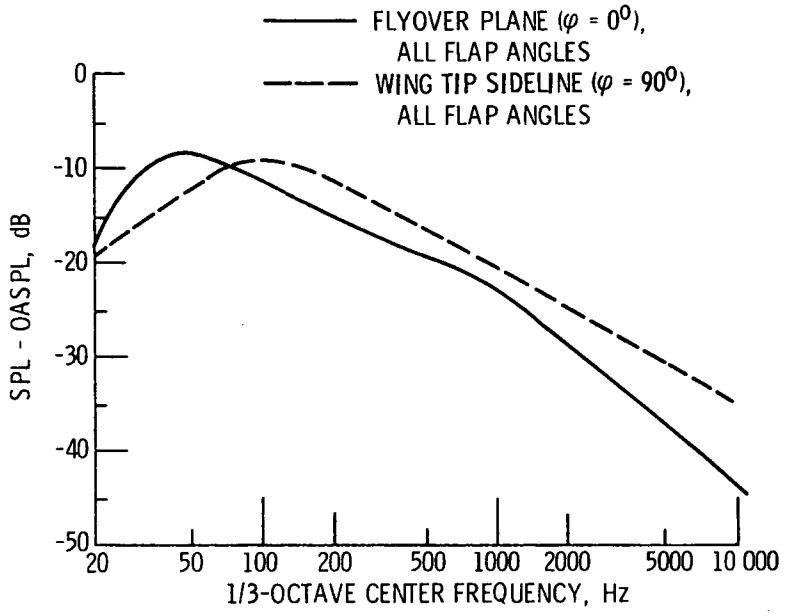

Figure 11. - Over-the-wing normalized flap noise spectra, scaled to nominal 25 000-pound thrust size (74-in. - equivalent nozzle diameter), for θ from 50° to 120°.

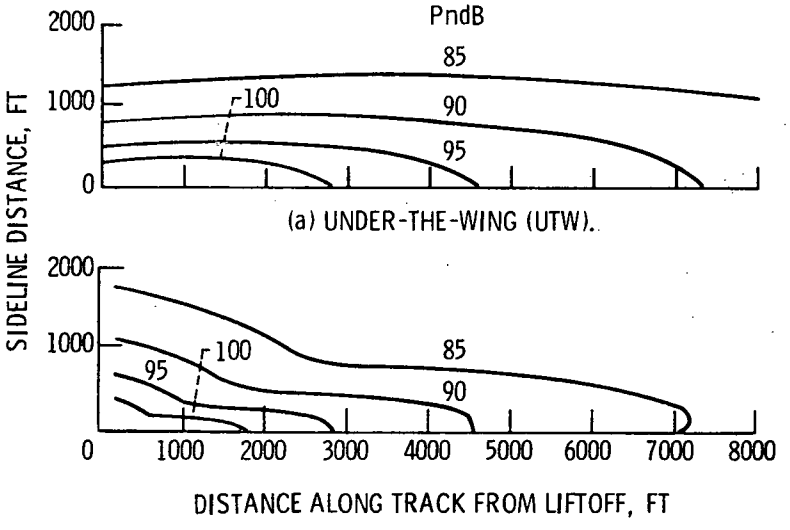

Figure 12. - Single engine flap noise footprints for UTW and OTW configurations. Flap angle of 30°, 10° climb angle, 10° angle of attack. UTW case: core velocity of 750 fps and area of 5.0 sq ft; fan velocity of 650 fps and area of 25.0 sq ft. OTW case: mixed velocity of 673 fps and total area of 30 sq ft. No installation effects, fuselage shielding, or extra ground attenuation included.